

Data Descriptor

A MODIS/ASTER Airborne Simulator (MASTER) Imagery for Urban Heat Island Research

Qunshan Zhao * and Elizabeth A. Wentz

GeoDa Center for Geospatial Analysis and Computation, School of Geographical Sciences and Urban Planning, Arizona State University, Tempe, AZ 85287-5302, USA; wentz@asu.edu

* Correspondence: qszhao@asu.edu; Tel.: +1-480-280-6586

Academic Editor: Juan C. Jiménez-Muñoz

Received: 24 April 2016; Accepted: 31 May 2016; Published: 6 June 2016

Abstract: Thermal imagery is widely used to quantify land surface temperatures to monitor the spatial extent and thermal intensity of the urban heat island (UHI) effect. Previous research has applied Landsat images, Advanced Spaceborne Thermal Emission and Reflection Radiometer (ASTER) images, Moderate Resolution Imaging Spectroradiometer (MODIS) images, and other coarse- to medium-resolution remotely sensed imagery to estimate surface temperature. These data are frequently correlated with vegetation, impervious surfaces, and temperature to quantify the drivers of the UHI effect. Because of the coarse- to medium-resolution of the thermal imagery, researchers are unable to correlate these temperature data with the more generally available high-resolution land cover classification, which are derived from high-resolution multispectral imagery. The development of advanced thermal sensors with very high-resolution thermal imagery such as the MODIS/ASTER airborne simulator (MASTER) has investigators quantifying the relationship between detailed land cover and land surface temperature. While this is an obvious next step, the published literature, *i.e.*, the MASTER data, are often used to discriminate burned areas, assess fire severity, and classify urban land cover. Considerably less attention is given to use MASTER data in the UHI research. We demonstrate here that MASTER data in combination with high-resolution multispectral data has made it possible to monitor and model the relationship between temperature and detailed land cover such as building rooftops, residential street pavements, and parcel-based landscaping. Here, we report on data sources to conduct this type of UHI research and endeavor to intrigue researchers and scientists such that high-resolution airborne thermal imagery is used to further explore the UHI effect.

Data Set: <http://dx.doi.org/10.6073/pasta/dd5f47bd551ee9bfd6e6105bd6c28fa> or <https://sustainability.asu.edu/caplter/data/data-catalog/view/knb-lter-cap.629.1/>

Data Set License: The data set is made available under a CC-BY license.

Keywords: MASTER; UHI; surface temperature; satellite thermal imagery; NAIP

1. Summary

With more than 50% of the world's population living in cities [1], a well-known phenomenon defined as the urban heat island (UHI) effect is negatively impacting human lives. As a result of the transformation of land surfaces and energy use, the UHI results in higher nighttime air and surface temperatures in urban areas compared to the surrounding rural areas [2–4]. The impact of the UHI includes increases in energy and water consumption, more intense heat waves during the summer, and higher risks of heat-related morbidity and mortality, particularly for young children, the aged, and low-income urban residents [5–9]. To understand the drivers of the UHI phenomenon and propose and implement mitigation effects, various methods are used to measure, monitor, and model the urban

land surface and air temperatures. Examples include *in-situ* field measurements [10], surface energy balance simulation [11], and satellite imagery derivation [12–16]. *In-situ* field measurements provide detailed and accurate surface and air temperature records, but the results are typically limited to a few discrete observations in small geographic areas rather than spatially continuous observations. Surface energy balance simulations apply urban energy balance models to predict urban surface temperatures based on surface properties and geometries, solar angles, and weather conditions. It provides continuous temperature estimates, but the simulation process is computationally expensive, which makes it difficult to extend the simulation to a large geographic area. Compared to *in-situ* field measurements and surface energy balance simulations, satellite thermal imagery provides rich spatial and temporal temperature information and serves as a complementary data source to other methods.

Various satellite imagery products provide the thermal infrared images for the land surface temperature derivation from low spatial resolution to high spatial resolution (see Table 1). Moderate Resolution Imaging Spectroradiometer (MODIS) images and Advanced Very High Resolution Radiometer (AVHRR) images have low spatial resolution (1000 m) but very high temporal resolution (one-day revisit time). They are widely used to detect temporal changes in the UHI effect at the regional or city level scale [15,17]. The Landsat Thematic Mapper (TM), Enhanced Thematic Mapper Plus (ETM+), Operational Land Imager/Thermal Infrared Sensor (OLI/TIRS) and Advanced Spaceborne Thermal Emission and Reflection Radiometer (ASTER) thermal imagery all have a moderate spatial resolution around 100 m. These data sources are widely used to understand seasonal or yearly changes of UHI effects across different land cover types because the temporal resolution of the thermal images is limited due to cloud cover and satellite revisit period (16 days) [18–21]. By combining TM, ETM+, and OLI/TIRS imagery, long-term time-series data to support longitudinal UHI research can be achieved with data sources of moderate spatial resolution [21]. Image fusion algorithms have been proposed to produce daily land surface temperature at Landsat resolution by fusing MODIS and Landsat data [22]. The image fusion algorithms make it possible to estimate moderate spatial resolution with high temporal-resolution thermal image products from existing satellite imagery. Although all of the data sets we mentioned here can be used to derive surface temperature and analyze UHI patterns, the resolution limitation makes it impossible to use these thermal images to quantify detailed variations in the UHI due to specific urban land cover or urban objects at fine spatial resolution.

Table 1. Remotely sensed thermal imagery used in urban heat island (UHI) research.

Satellite (Sensor)	Spatial Resolution (Thermal Band)	Revisit Time (Days)	Years of Operation
Low spatial resolution			
NOAA (AVHRR)	1000 m	1	1979 to present
EOS (MODIS)	1000 m	1	1999 to present
Moderate spatial resolution			
Landsat (TM)	120 m	16	1984–2011
Landsat (ETM+)	60 m	16	1999 to present
Landsat (OLI/TIRS)	100 m	16	2013 to present
EOS (ASTER)	90 m	(on demand)	1999 to present
High spatial resolution			
Airborne (MASTER)	Depending on flight height (5–50 m)	(on demand)	1998 to present
Airborne (HyTES)	Depending on flight height (3.41 m with 2000 flight altitude)	(on demand)	2013 to present

The MODIS/ASTER airborne simulator (MASTER) instrument has provided high-resolution (5–50 m) hyperspectral imagery since 1998 [23]. MASTER was developed to obtain a higher-spatial-resolution imagery in order to compare spaceborne data set (MODIS and ASTER) and *in-situ* field measurements. The MASTER instrument is carried by the King Air Beachcraft B200 aircraft from Department of Energy. The imagery has 50 spectral bands, which measure the visible wavelengths through mid-infrared wavelengths (0.46–12.817 μm). As a hyperspectral image, MASTER images are widely used for applications such as discriminating burned areas [24], land cover classification [25],

and coral reef habitat mapping [26]. However, there is limited usage of the high-resolution thermal bands of MASTER to analyze UHI patterns and phenomena in urban areas.

With the availability of high-resolution thermal imagery from MASTER, researchers are able to study environmental urban processes at a fine spatial resolution, such as landscape and climate modification, surface energy balance, evapotranspiration, and the societal implications of the UHI. For example, Stefanov *et al.* [27] investigated the human modifications of climate and landscape by using MASTER data in Phoenix metropolitan area. Social survey data such as ethnicity groups and income level were used to make correlations with neighborhood temperature. Research outcomes explained that inequity existed in the microclimate experience of Phoenix residents. Jenerette *et al.* [14] analyzed MASTER imagery with a social survey to investigate residential neighborhoods and parcel scale temperature variations under different land cover and landscapes. Results showed that vegetation was effective at cooling residential neighborhoods, and heat-related illness was correlated with daytime surface temperature at parcel level. Zhao *et al.* [28] utilized MASTER, Quickbird, and Light Detection and Ranging (LIDAR) data to explore the relationships among rooftop surface temperature, rooftop configuration, and nearby outdoor landscaping. The results demonstrated that outdoor landscaping and rooftop albedo significantly contributed to lower daytime rooftop surface temperatures. Vanos *et al.* [29] compared MASTER surface temperature with *in-situ* urban surface temperature to explore the relationships between hot playgrounds and children's health in Gilbert, Arizona. MASTER data proved to be a valuable complementary data source to represent the playground temperature. These examples illustrate the research opportunities that MASTER thermal infrared imagery serves as the data source for researchers to conduct micro-level urban surface temperature analysis.

2. Data Description

The data reported here were collected from the MASTER superspectral sensor that flew over the Phoenix metropolitan area on 12–13 July (daytime) and 15–16 July (nighttime). The spatial resolution is ~7 m/pixel. There are small variations in the pixel size due to distortion. Figure 1 shows the MASTER nighttime temperature imagery of our study area in Tempe, Arizona, USA. We generated this data set by applying atmospheric and geometric correction, then reducing the spatial extent to the specific study area. Our research focused on a residential neighborhood with mostly single family parcels. The MASTER data described in this paper were used to support the rooftop analysis reported by Zhao *et al.* (2015) [28].

In our data set (see Figure 1), major roads exhibit the highest surface temperature (red), followed by residential roads/pavement (orange) and household parcel/urban parks (green). The raster cells with the minimum temperature values (white pixels in Figure 1) are small clouds in the sky. These cells need to be removed before using the MASTER data set.

Table 2 provides a summary of the final data set characteristics of the MASTER nighttime image shown in Figure 1. The data are a single IMAGINE Image referenced in a latitude/longitude grid with a file size of 3.45 MB. This image was collected on 15th July 2011 (15.7.2011) with the pixel value reported in degrees Celsius (°C). The nighttime data ranged from 2.96 to 35.37 °C, with the mean of 23.94 °C and standard deviation of 3.68 °C.

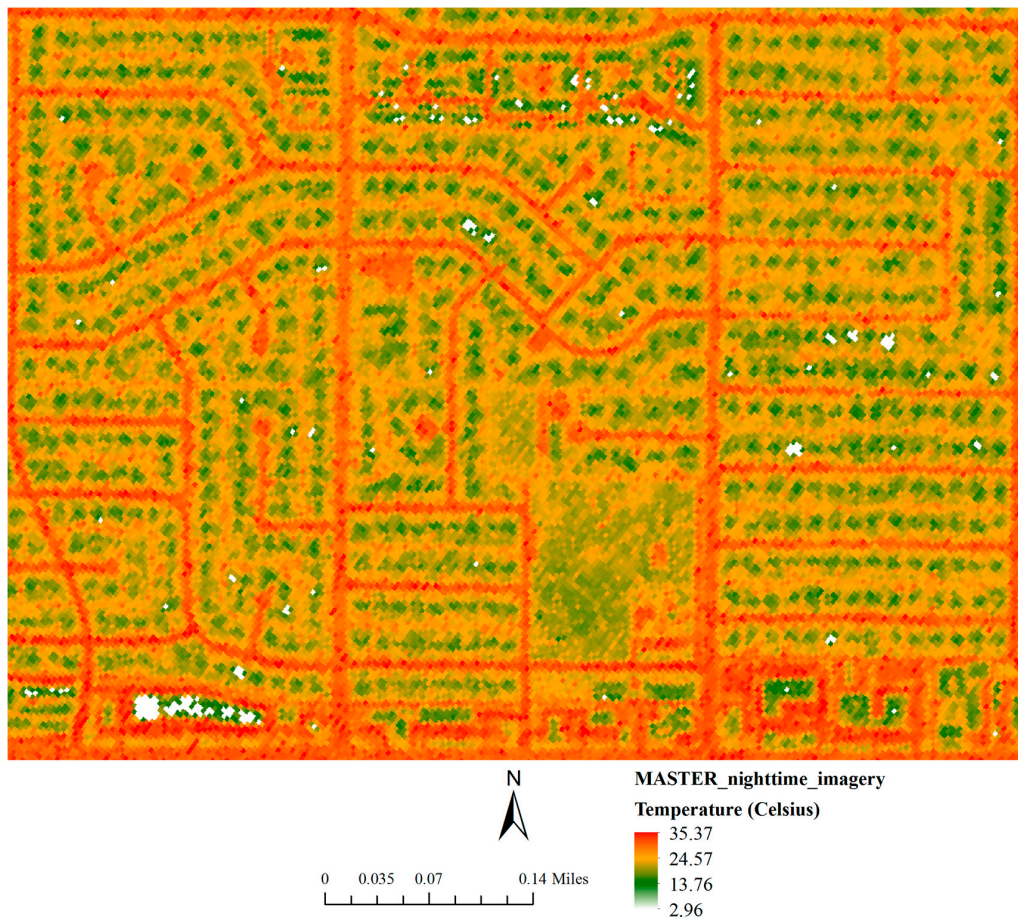


Figure 1. MASTER nighttime temperature imagery in the study area.

Table 2. Data set characteristics of the MASTER nighttime temperature layer 2011.

Characteristic	Description
Data format	IMAGINE Image
Epoch	15 July 2011
Coordinate system and projection	NAD_1983_UTM_Zone_12N
Image dimensions	1106 × 817 (columns × rows)
Size	3.45 MB
Number of layers	1
Value	Land surface temperature in Celsius
Maximum value	35.37
Minimum value	2.96
Mean value	23.94
Value of standard deviation	3.68

3. Materials and Methods

3.1. Raw MASTER and Reference Imagery

Any of the raw MASTER L1B and L2 level data (without atmospheric and geometric correction) can be freely downloaded from MASTER's official website at National Aeronautics and Space Administration (NASA) [30]. The raw MASTER imagery used in Zhao *et al.* (2015) [28] was downloaded from the NASA website for the Phoenix area [31] (see Figure 2). Because the original MASTER data does not include any geolocation information and includes distorted areas due to the aircraft wobble, high-quality reference imagery is required for geometric correction.

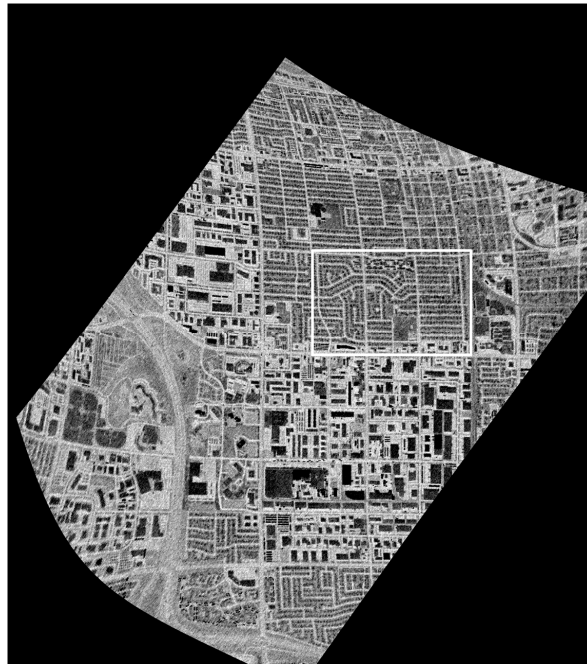


Figure 2. Raw MASTER nighttime imagery. Outline defines the study area for the research and the portion of the data used for analysis.

For the Phoenix metropolitan area, we used the National Agriculture Imagery Program (NAIP) data as the reference imagery. NAIP data are 1-meter orthorectified images collected by the United States Department of Agriculture (USDA) during the agricultural growing season in the United States. NAIP imagery has a combination of four multispectral bands (blue, green, red, and near-infrared bands). While NAIP focuses on agricultural areas, the USDA extends the data collection to cover the complete state. All the NAIP images can be freely downloaded from the USDA website [32]. These data are ideal for georeferencing MASTER data because the pixel size and feature discrimination are similar to the MASTER imagery. Figure 3 illustrates the NAIP imagery used for geometric correction in our study area.

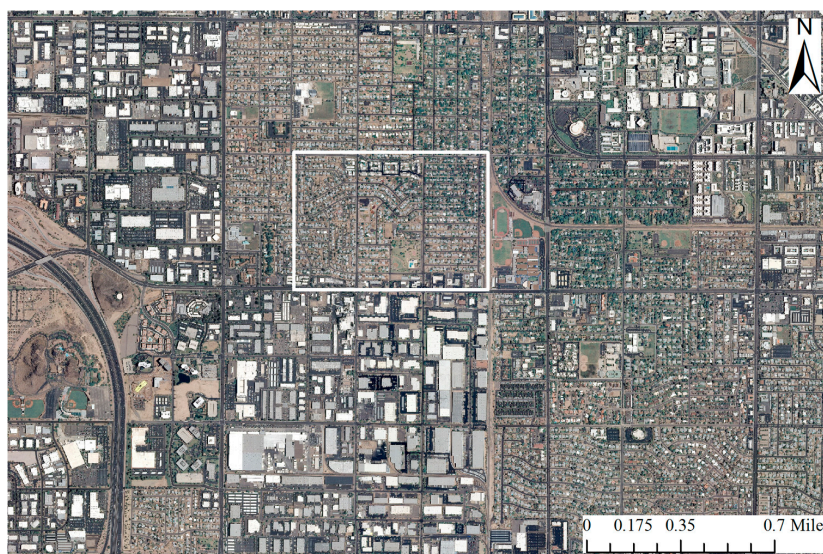


Figure 3. NAIP imagery. Outline defines the study area for the research and the portion of the data used for analysis.

3.2. Atmospheric and Geometric Correction

The MASTER thermal infrared data (temperature) were atmospherically corrected by using an in-scene atmospheric compensation (ISAC) technique. This involved separating the emissivity and surface temperature with an emissivity normalization approach [33–37] using the basic version of ENVI/IDL software (Exelis Visual Information Solutions, Boulder, CO, USA).

After importing MASTER thermal infrared bands into ENVI/IDL software, the raw radiance was scaled to $W/m^2/\mu m/sr$. To apply ISAC algorithm, the assumption is a near-blackbody surface exists in the scene and the atmosphere is uniform all over the data scene. After running the ISAC algorithm, per pixel values for emissivity and surface temperature were derived. A detailed description and mathematical equations of the ISAC algorithm can be found at Young *et al.* (2002) [37]. Then, an emissivity normalization method was utilized to separate surface temperature and emissivity of the thermal infrared bands. This method calculates the temperature for every band and pixel by using a fixed emissivity value.

The MASTER data were geometrically corrected using an image warping approach with the second-order polynomial nearest neighbor resampling method, also completed with the basic version of ENVI/IDL. We manually identified 80 ground control points in both the MASTER image and NAIP image to geometrically align the MASTER image with the NAIP. In the end, the MASTER nighttime imagery was geographically referenced with a root-mean-square (RMS) error of 0.26 m.

4. User Notes

All the georeferenced MASTER image and other related data set from Zhao *et al.* (2015) [28] are available at United States Long-Term Ecological Research (LTER) network data portal [38] and Central Arizona-Phoenix Long-Term Ecological Research (CAPLTER) data portal [39]. The data are available for use, but careful attention should be given to the distortion areas and cloud pixels.

Other MASTER images are available for downloading and processing for analyzing the thermal dynamics in urban areas. The key points here serve to guide users in processing these images in other geographical settings. First, because the MASTER images are acquired by aircraft with different flight heights and under different weather conditions, it is important to check the metadata before processing and applying the MASTER image. The metadata describe flight conditions needed for data processing. Second, sensor limitation and data acquisition through aircraft results in warping particularly along the edges of the data set. Consequently, careful selection of both MASTER data and high-resolution geographically referenced data are critical for accurate geometric correction.

5. Conclusions

With the availability of high-resolution multispectral remotely sensed imagery and detailed social and health survey data, MASTER images can serve as an important surface temperature data source to analyze UHI effects with health conditions, water usage, energy consumption, and various social factors. The aim of this paper is to attract geographers, sociologist, urban planners, and remote sensing scientists' attention of using MASTER data set in their urban heat related research. Detailed neighborhood-level understanding of urban heat and heat-related problems can be analyzed with MASTER data. In a desert city such as Phoenix, Arizona, the tradeoff between water usages, outdoor landscaping design (xeric or mesic landscape), energy saving, and UHI mitigation is a long-standing research area for creating a sustainable desert community. Future work will focus on using MASTER imagery to analyze the temperature variation in the residential parcels under different vegetation conditions, and explore the optimal outdoor landscaping design with the best heat mitigation and water efficiency. Further, combining social and health survey data with MASTER temperature data will identify more research opportunities for understanding urban heat within different community demography conditions and social inequity.

Acknowledgments: This material is based upon work supported by the National Science Foundation under Grant SES-0951366, Decision Center for a Desert City II: Urban Climate Adaptation. The acquisition and processing of the MASTER data was supported by the National Science Foundation under Grant BCS-1026865: Central Arizona-Phoenix Long-Term Ecological Research and GEO-0816168: Urban Vulnerability to Climate Change. Qunshan Zhao is partly supported by the Graduate Grant of the Central Arizona-Phoenix Long-Term Ecological Research and the National Natural Science Foundation of China (No. 51378399 and 41331175). Any opinions, findings, and conclusions or recommendations expressed in this material are those of the authors and do not necessarily reflect the views of the National Science Foundation. The authors also want to thank Jessica Jia for processing MASTER imagery and the anonymous reviewers for their valuable comments and suggestions to improve the manuscript.

Author Contributions: Both authors contribute to the research and analysis of the data, as well as writing this article.

Conflicts of Interest: The authors declare no conflict of interest.

Abbreviations

The following abbreviations are used in this manuscript:

NOAA	National Oceanic and Atmospheric Administration
NASA	National Aeronautics and Space Administration
EOS	Earth Observing System
USDA	United States Departments of Agriculture
TM	Thematic Mapper
ETM+	Enhanced Thematic Mapper Plus
OLI/TIRS	Operational Land Imager/Thermal Infrared Sensor
MODIS	Moderate Resolution Imaging Spectroradiometer
AVHRR	Advanced Very High Resolution Radiometer
MASTER	MODIS/ASTER airborne simulator
HyTES	Hyperspectral Thermal Emission Spectrometer
NAIP	National Agriculture Imagery Program
LIDAR	Light Detection and Ranging
UHI	Urban Heat Island
ASTER	Advanced Spaceborne Thermal Emission and Reflection Radiometer
ISAC	In-scene Atmospheric Compensation

References

1. United Nations. *World Urbanization Prospects: The 2014 Revision*; United Nations, Department of Economic and Social Affairs & Population Division: New York, NY, USA, 2014.
2. Bornstein, R.D. Observations of the urban heat island effect in New York City. *J. Appl. Meteorol.* **1968**, *7*, 575–582. [[CrossRef](#)]
3. Kim, H.H. Urban heat island. *Int. J. Remote Sens.* **1992**, *13*, 2319–2336. [[CrossRef](#)]
4. Oke, T.R. The energetic basis of the urban heat island. *Q. J. R. Meteorol. Soc.* **1982**, *108*, 1–24. [[CrossRef](#)]
5. Bassil, K.L.; Cole, D.C. Effectiveness of Public Health Interventions in Reducing Morbidity and Mortality during Heat Episodes: A Structured Review. *Int. J. Environ. Res. Public Health* **2010**, *7*, 991–1001. [[CrossRef](#)] [[PubMed](#)]
6. Bi, P.; Williams, S.; Loughnan, M.; Lloyd, G.; Hansen, A.; Kjellstrom, T.; Dear, K.; Saniotis, A. The Effects of Extreme Heat on Human Mortality and Morbidity in Australia: Implications for Public Health. *Asia. Pac. J. Public Health* **2011**. [[CrossRef](#)]
7. Harlan, S.L.; Brazel, A.J.; Prashad, L.; Stefanov, W.L.; Larsen, L. Neighborhood microclimates and vulnerability to heat stress. *Soc. Sci. Med.* **2006**, *63*, 2847–2863. [[CrossRef](#)] [[PubMed](#)]
8. McGeehin, M.A.; Mirabelli, M. The potential impacts of climate variability and change on temperature-related morbidity and mortality in the United States. *Environ. Health Perspect.* **2001**, *109*, 185–189. [[CrossRef](#)] [[PubMed](#)]
9. Tomlinson, C.J.; Chapman, L.; Thornes, J.E.; Baker, C.J. Including the urban heat island in spatial heat health risk assessment strategies: A case study for Birmingham, UK. *Int. J. Health Geogr.* **2011**, *10*. [[CrossRef](#)] [[PubMed](#)]
10. Stoll, M.J.; Brazel, A.J. Surface-air temperature relationships in the urban environment of Phoenix, Arizona. *Phys. Geogr.* **1992**, *13*, 160–179.

11. Krayenhoff, E.S.; Voogt, J.A. A microscale three-dimensional urban energy balance model for studying surface temperatures. *Bound.-Layer Meteorol.* **2007**, *123*, 433–461. [[CrossRef](#)]
12. Myint, S.W.; Wentz, E.A.; Brazel, A.J.; Quattrochi, D.A. The impact of distinct anthropogenic and vegetation features on urban warming. *Landsc. Ecol.* **2013**, *28*, 959–978. [[CrossRef](#)]
13. Fan, C.; Myint, S.W.; Zheng, B. Measuring the spatial arrangement of urban vegetation and its impacts on seasonal surface temperatures. *Prog. Phys. Geogr.* **2015**, *39*, 199–219. [[CrossRef](#)]
14. Jenerette, G.D.; Harlan, S.L.; Buyantuev, A.; Stefanov, W.L.; Decler-Barreto, J.; Ruddell, B.L.; Myint, S.W.; Kaplan, S.; Li, X. Micro-scale urban surface temperatures are related to land-cover features and residential heat related health impacts in Phoenix, AZ USA. *Landsc. Ecol.* **2016**, *31*, 745–760. [[CrossRef](#)]
15. Tran, H.; Uchiyama, D.; Ochi, S.; Yasuoka, Y. Assessment with satellite data of the urban heat island effects in Asian mega cities. *Int. J. Appl. Earth Obs. Geoinform.* **2006**, *8*, 34–48. [[CrossRef](#)]
16. Zhang, X.; Aono, Y.; Monji, N. Spatial Variability of Urban Surface Heat Fluxes Estimated from Landsat TM Data under Summer and Winter Conditions. *J. Agric. Meteorol.* **1998**, *54*, 1–11. [[CrossRef](#)]
17. Gallo, K.P.; McNab, A.L.; Karl, T.R.; Brown, J.F.; Hood, J.J.; Tarpley, J.D. The use of NOAA AVHRR data for assessment of the urban heat island effect. *J. Appl. Meteorol.* **1993**, *32*, 899–908. [[CrossRef](#)]
18. Chen, X.-L.; Zhao, H.-M.; Li, P.-X.; Yin, Z.-Y. Remote sensing image-based analysis of the relationship between urban heat island and land use/cover changes. *Remote Sens. Environ.* **2006**, *104*, 133–146. [[CrossRef](#)]
19. Zhang, H.; Qi, Z.; Ye, X.; Cai, Y.; Ma, W.; Chen, M. Analysis of land use/land cover change, population shift, and their effects on spatiotemporal patterns of urban heat islands in metropolitan Shanghai, China. *Appl. Geogr.* **2013**, *44*, 121–133. [[CrossRef](#)]
20. Sun, R.; Chen, L. How can urban water bodies be designed for climate adaptation? *Landsc. Urban Plan.* **2012**, *105*, 27–33. [[CrossRef](#)]
21. Shen, H.; Huang, L.; Zhang, L.; Wu, P.; Zeng, C. Long-term and fine-scale satellite monitoring of the urban heat island effect by the fusion of multi-temporal and multi-sensor remote sensed data: A 26-year case study of the city of Wuhan in China. *Remote Sens. Environ.* **2016**, *172*, 109–125. [[CrossRef](#)]
22. Weng, Q.; Fu, P.; Gao, F. Generating daily land surface temperature at Landsat resolution by fusing Landsat and MODIS data. *Remote Sens. Environ.* **2014**, *145*, 55–67. [[CrossRef](#)]
23. Hook, S.J.; Myers, J.J.; Thome, K.J.; Fitzgerald, M.; Kahle, A.B. The MODIS/ASTER airborne simulator (MASTER)—A new instrument for earth science studies. *Remote Sens. Environ.* **2001**, *76*, 93–102. [[CrossRef](#)]
24. Veraverbeke, S.; Harris, S.; Hook, S. Evaluating spectral indices for burned area discrimination using MODIS/ASTER (MASTER) airborne simulator data. *Remote Sens. Environ.* **2011**, *115*, 2702–2709. [[CrossRef](#)]
25. Li, P.; Moon, W.M. Land cover classification using MODIS–ASTER airborne simulator (MASTER) data and NDVI: A case study of the Kochang area, Korea. *Can. J. Remote Sens.* **2004**, *30*, 123–126. Available online: http://www.tandfonline.com/doi/abs/10.5589/m03-061#.VxU_avkrIuU (accessed on 18 April 2016). [[CrossRef](#)]
26. Capolsini, P.; Andréfouët, S.; Rion, C.; Payri, C. A comparison of Landsat ETM+, SPOT HRV, Ikonos, ASTER, and airborne MASTER data for coral reef habitat mapping in South Pacific islands. *Can. J. Remote Sens.* **2003**, *29*, 187–200. [[CrossRef](#)]
27. Stefanov, W.L.; Prashad, L.; Eisinger, C.; Brazel, A.; Harlan, S.L. Investigation of human modifications of landscape and climate in the Phoenix Arizona Metropolitan area using MASTER data. *Pan* **2004**, *2*, 2–8.
28. Zhao, Q.; Myint, S.W.; Wentz, E.A.; Fan, C. Rooftop Surface Temperature Analysis in an Urban Residential Environment. *Remote Sens.* **2015**, *7*, 12135–12159. [[CrossRef](#)]
29. Vanos, J.K.; Middel, A.; McKercher, G.R.; Kuras, E.R.; Ruddell, B.L. Hot playgrounds and children’s health: A multiscale analysis of surface temperatures in Arizona, USA. *Landsc. Urban Plan.* **2016**, *146*, 29–42. [[CrossRef](#)]
30. MASTER—The MODIS/ASTER Airborne Simulator. Available online: <http://master.jpl.nasa.gov/> (accessed on 1 June 2016).
31. MASTER—Level-1B Available Data Flight #11-004-04. Available online: <http://master.jpl.nasa.gov/data/MissionView.htm?Missionid=100796> (accessed on 1 June 2016).
32. United States Department of Agriculture Geospatial Data Gateway. Available online: <https://gdg.sc.egov.usda.gov/> (accessed on 1 June 2016).

33. Kealy, P.S.; Hook, S.J. Separating temperature and emissivity in thermal infrared multispectral scanner data: Implications for recovering land surface temperatures. *IEEE Trans. Geosci. Remote Sens.* **1993**, *31*, 1155–1164. [[CrossRef](#)]
34. Johnson, B.R.; Young, S.J. *In-Scene Atmospheric Compensation: Application to SEBASS Data Collected at the ARM Site*; Space and Environment Technology Center, The Aerospace Corporation: Los Angeles, CA, USA, 1998.
35. Hernandez-Baquero, E.D. Characterization of the Earths Surface and Atmosphere from Multispectral and Hyperspectral Thermal Imagery. Ph.D. Thesis, Rochester Institute of Technology, Chester F. Carlsom Center for Imaging Science, Rochester, NY, USA, 2000.
36. Hook, S.J.; Gabell, A.R.; Green, A.A.; Kealy, P.S. A comparison of techniques for extracting emissivity information from thermal infrared data for geologic studies. *Remote Sens. Environ.* **1992**, *42*, 123–135. [[CrossRef](#)]
37. Young, S.J.; Johnson, B.R.; Hackwell, J.A. An in-scene method for atmospheric compensation of thermal hyperspectral data. *J. Geophys. Res.* **2002**, *107*. [[CrossRef](#)]
38. Zhao, Q. Analysis of Rooftop Surface Temperatures in an Urban Residential Environment. Long Term Ecological Research Network. Available online: <http://dx.doi.org/10.6073/pasta/dd5f47bd551ee9bfdd6e6105bd6c28fa> (accessed on 2 June 2016).
39. Central Arizona-Phoenix Long-Term Ecological Research Data Catalog—Analysis of rooftop surface temperatures in an urban residential environment. Available online: <https://sustainability.asu.edu/capltter/data/data-catalog/view/knb-lter-cap.629.1/> (accessed on 1 June 2016).



© 2016 by the authors; licensee MDPI, Basel, Switzerland. This article is an open access article distributed under the terms and conditions of the Creative Commons Attribution (CC-BY) license (<http://creativecommons.org/licenses/by/4.0/>).